Tissue, system and organ physiology

Glutamatergic, cholinergic and GABAergic neurons contribute to the septohippocampal pathway and exhibit distinct electrophysiological properties: novel implications for hippocampal rhythmicity.

F. Sotty, M. Danik, F. Manseau, F. Laplante, R. Quirion and S. Williams*.

Douglas Hospital Research Center
Dept of Psychiatry, McGill University
6875, Lasalle Blvd
Montreal, Quebec, H4H 1R3, CANADA.

Abbreviated title: Electrophysiology of identified MSDB neurons.

Number of text pages: 40; Number of figures: 8; Number of table: 1; Number of words in the Abstract: 250; Introduction: 531; Discussion: 1664.

Correspondence should be addressed to Dr. Sylvain Williams: Tel: (+1) 514 761 6131 ext. 5937; Fax: (+1) 514 762 3034; wilsyl@douglas.mcgill.ca.

Acknowledgements: This work was supported by the Canadian Institute of Health Research (CIHR), the Natural Sciences and Engineering Research Council of Canada (NSERC) and Alzheimer Society of Canada. FS was supported by a fellowship from the Fonds de la Recherche en Santé du Québec (FRSQ).

Keywords: septohippocampal pathway; cholinergic neurons; GABAergic neurons; glutamatergic neurons; hyperpolarization-activated current; theta rhythm.

ABSTRACT

The medial septum – diagonal band complex (MSDB) contains cholinergic and non-cholinergic neurons known to play key roles in learning and memory processing, and in the generation of hippocampal theta rhythm. Electrophysiologically, several classes of neurons have been described in the MSDB, but their chemical identity remains to be fully established. By combining electrophysiology to single-cell RT-PCR, we have identified 4 classes of neurons in the MSDB *in vitro*. The first class displayed slow-firing, little or no I_h, and expressed choline acetyl-transferase mRNA (ChAT). The second class was fast-firing, had an important I_h and expressed glutamic acid decarboxylase 67 mRNA (GAD67), sometimes co-localized with ChAT mRNAs. A third class exhibited fast- and burst-firing, an important I_h, expressed GAD67 mRNA also occasionally co-localized with ChAT mRNAs. The ionic mechanism underlying the bursts involved a low-threshold spike and a prominent I_h current, conductances often associated with pacemaker activity. Interestingly, we identified a fourth class that expressed transcripts solely for one or two of the vesicular glutamate transporter (VGLUT1 and VGLUT2), but not ChAT or GAD. Some putative glutamatergic neurons displayed electrophysiological properties similar to ChAT-positive slow-firing neurons such as the occurrence of a very small I_h, however nearly half of glutamatergic neurons exhibited cluster firing with intrinsically generated voltage-dependent subthreshold membrane oscillations. Neurons belonging to each of the four described classes were found among septohippocampal neurons by retrograde labelling. We provide results suggesting that slow-firing cholinergic, fast-firing and burst-firing GABAergic, and cluster-firing glutamatergic neurons, may each uniquely contribute to hippocampal rhythmicity *in vivo*.

It is now well established that the medial septum-diagonal band complex (MSDB) is involved in generating hippocampal theta rhythm, as well as in learning and memory processing (Bland and Oddie, 2001; Buzsaki, 2002; Stewart and Fox, 1990). The MSDB comprises a heterogeneous number of neurons, including cholinergic and non-cholinergic neurons, both providing projections to the hippocampus (Freund, 1989; Freund and Antal, 1988). Although the cholinergic component could provide an important tonic increase in hippocampal excitability, non-cholinergic neurons may be the pacemaker generating hippocampal theta rhythm (Apartis et al., 1998; Brazhnik and Fox, 1997; King et al., 1998; Lee et al., 1994; Toth et al., 1997).

Electrophysiological studies have identified slow-firing, fast-firing, burst-firing, and cluster-firing neurons in the MSDB (Gorelova and Reiner, 1996; Griffith et al., 1988; Jones et al., 1999; Serafin et al., 1996) based on characteristics such as the maximum firing frequency, the prominence of an hyperpolarization-activated current (I_h) and duration of the after-hyperpolarizing potential (AHP). Slow-firing neurons correspond to septohippocampal cholinergic neurons (Alreja et al., 2000; Gorelova and Reiner, 1996; Griffith and Matthews, 1986; Markram and Segal, 1990). In contrast, the phenotype of fast-firing, burst-firing, and cluster-firing non-cholinergic neurons remains unclear. Fast-firing neurons were shown to express parvalbumin (Morris et al., 1999; Morris and Henderson, 2000), a calcium-binding protein expressed in most GABAergic neurons (Freund, 1989; Freund and Antal, 1988; Gritti et al., 2003), as well as GAD67 mRNA (Knapp et al., 2000), suggesting that a majority of fast-firing neurons may be GABAergic. The phenotype of burst-firing and cluster-firing neurons has not yet been determined, but possibilities include that they are GABAergic, or express a neurotransmitter distinct from ACh or GABA, such as glutamate, as recently suggested by some studies (Gritti et al., 1997; Kiss et al., 2002; Manns et al., 2001; Gritti et al., 2003).

Although non-cholinergic neurons seem critical in generating hippocampal theta rhythm (Apartis et al., 1998; Brazhnik and Fox, 1997; King et al., 1998; Lee et al., 1994), the precise electrophysiological mechanisms underlying pacemaker activity remain unknown. In this respect, the important expression of the pacemaker current I_h in the MSDB would be relevant, since it is known to contribute to the expression of rhythmic bursting and network oscillations in various brain areas (Dickson et al., 2000; Lüthi et al, 1998; Lüthi and McCormick, 1998; Maccaferi and McBain, 1996; Pape, 1996; Thoby-Brisson et al., 2000). In agreement with this proposal, preliminary evidence suggests that selective I_h blockade in the MSDB disrupts hippocampal theta activity *in vivo* (Xu et al., 2002). It remains to be determined which MSDB neuronal phenotype expresses a sufficiently important I_h to potentially sustain pacemaker activity. The purpose of the present study was: i) to determine the phenotype of electrophysiologically characterized MSDB neurons *in vitro* by combining whole-cell recordings to single-cell (sc) reverse transcription (RT-PCR), ii) to examine which of these electrophysiologically characterized neuronal classes are septohippocampal neurons, and iii) to determine which neuronal population(s) express I_h current, and how it contributes to firing properties.

The present study reveals that the MSDB contains septohippocampal cholinergic, GABAergic and glutamatergic neurons. GABAergic, and newly identified glutamatergic neurons, have intrinsic firing properties that may confer them an important role in pacing the hippocampus *in vivo*.

MATERIALS AND METHODS

Slice preparation. Brain slices containing the MSDB were obtained from Sprague-Dawley rats (13-19 days old, Charles River Canada, St Constant, Quebec). Animal care was provided according to protocols and guidelines approved by McGill University and the Canadian Council of Animal Care. Rats were killed by decapitation and the brain was rapidly removed and placed in ice-cold artificial cerebrospinal fluid (ACSF), pH 7.4, equilibrated with 95% O_2 / 5% CO_2, containing (in mM): 126 NaCl, 24 $NaHCO_3$, 10 glucose, 3 KCl, 2 $MgSO_4$, 1.25 NaH_2PO_4 and 2 $CaCl_2$. Coronal slices of 350 μm thickness containing the MSDB were cut with a Vibroslice (Campden Instruments Ltd., UK) and placed in a Petri dish containing oxygenated ACSF. After 1 to 1.5 h, the slice was transferred to a Plexiglas recording chamber on the stage of a Nikon microscope (Eclipse E600FN) equipped with Nomarsky optics, and continuously perfused with ACSF at a rate of 1-2 ml/min for electrophysiological recordings. Cells were visualized using a 40X water immersion objective.

Whole-cell recordings. Patch pipettes (3-6 MΩ) were pulled from heat-sterilized borosilicate glass capillary tubing (Warner Instrument Corp., Hamden, CT, USA) and filled with 6 μl of internal solution prepared with nuclease-free water (Sigma, Oakville, On, Canada) containing (in mM): 144 potassium gluconate, 3 $MgCl_2$, 0.2 EGTA, 10 HEPES, and 0.3 Tris-GTP, pH 7.2 (285/295 mOsm). Whole-cell recordings in voltage-clamp and current-clamp modes were performed at room temperature using a whole-cell patch-clamp amplifier PC-505A (Warner Instrument Corp., Hampden, CT, USA). The junction potential estimated at -14 mV was not corrected unless otherwise indicated. The output signal was continuously filtered at 2 kHz. Data

were digitized and analyzed using pClamp 8.0.1 software (Axon instruments, Union City, CA, USA).

Electrophysiological analysis. The resting membrane potential was measured in current-clamp mode once a stable recording was obtained. The protocol was continued only when the resting membrane potential was more negative than -45 mV, spikes overshot 0 mV and the series resistance was less than 30 MΩ. In current-clamp mode, the membrane potential of each cell was first held at -60 mV and a series of hyperpolarizing and depolarizing current pulses (0-200 pA, 1-4 s) was applied. The membrane was then held at -80 mV and the same series of depolarizing pulses was applied. For each neuron, the presence of a voltage-dependent inward rectification (depolarizing sag) in response to series of 4s-hyperpolarizing current pulses was noted, and its amplitude was measured for the current pulse inducing an initial hyperpolarization to –95 mV. Firing properties were analyzed in response to series of 1-8 s-depolarizing current pulses applied from –60 mV, and then repeated from a membrane potential of –80 mV. Firing frequencies were determined for each neuron depolarized from –60 mV, using the same current pulse required to depolarize the cell to threshold from –80 mV (Jones et al., 1999). Maximal firing frequency was calculated from the time interval between the first and the second spike in a train evoked by a 1s-depolarizing current pulse, steady firing frequency was calculated from the time interval between the last 2 spikes in a train evoked by a 1s-depolarizing current pulse, mean firing rate was calculated from the number of spikes evoked by a 1s-depolarizing current pulse. Spike accommodation was measure using a 1 s depolarizing step by calculating (firing frequency during the first 200ms - the firing frequency during the last 200ms)/frequency of first 200ms. In voltage-clamp mode, the presence of the hyperpolarization-activated current (I_h) was determined

by applying a series of 2 s long hyperpolarizing voltage steps of increasing amplitude from -50 to -120 mV. The currents evoked by injection of hyperpolarizing voltage steps revealed two components: an initial instantaneous change in membrane conductance (instantaneous current) and a secondary slowly developing inward current (steady-state current), that closely resembled the I_h current described previously (Pape, 1996). The amplitude of I_h current corresponded to the difference between the amplitude of the steady-state current and instantaneous current, and was represented by plotting the instantaneous and steady state currents as a function of membrane voltage. The activation time constant of I_h current ($T_{1/2}$) was determined for a voltage step from –50 to –120 mV, and corresponded to the time required from the activation of the instantaneous current to reach half of the steady-state current amplitude.

Cytoplasm harvest and reverse transcription. At the end of each recording, the cell content was aspirated under visual control by applying a gentle negative pressure in the patch pipette. The series resistance and leak current were monitored throughout the aspiration procedure and the negative pressure was interrupted before or as soon as the seal was lost. The pipette was then quickly removed from the slice, and its content was expelled in a 0.2 ml PCR tube containing 15U ribonuclease inhibitor (Takara Biomedicals, Otsu, Japan) and 8.3 mM dithiothreitol (DTT, Sigma), and quickly cooled on ice. Fifty picomoles of random hexamers (Applied Biosystems, Foster City. CA, USA) were added, the volume was measured and adjusted to 12.5 µl with nuclease-free water. The tube was heated for 1 min to 95°C and quickly cooled on ice. First strand cDNA was synthesized using 100 U SuperScript II RnaseH Reverse Transcriptase (Invitrogen, Rockville, MD, USA) for 2h at 42°C / overnight at 37°C after an initial incubation for 10 min at room temperature in a total reaction volume of 20 µl containing 1X First Strand Buffer (50 mM Tris-HCl pH 8.3, 75 mM KCl, 3 mM $MgCl_2$; Invitrogen), 0.5 mM dNTPs (Life

Technologies), and freshly added 10 mM DTT and 20 U ribonuclease inhibitor. The reverse transcriptase was denaturated at 70°C for 15 min and RNA was removed by incubation with 2 U Ribonuclease H (Takara Biomedicals) for 20 min at 37°C. The single-cell cDNA was stored at -80°C until PCR amplification.

Multiplex PCR. A two-step PCR protocol, slightly modified from that described by Ruano et al. (1995) and Puma et al., (2001), was used for the amplification of cDNAs for choline acetyltransferase (ChAT), glutamic acid decarboxylases 65 and 67 (GAD65 and GAD67), and vesicular glutamate transporters 1 and 2 (VGLUT1 and VGLUT2), reported to be specifically expressed in glutamatergic neurons (Fujiyama et al., 2001; Takamori et al., 2001). The first-round PCR reaction was performed in a final volume of 100 µl containing the 21 µl RT reaction, 10 pmoles of each selected primer, 50 µM of each dNTPs, 2 mM $MgCl_2$, 1X PCR Buffer II (50 mM KCl, 10 mM Tris-HCl, pH 8.3) and 2.5 U AmpliTaq DNA Polymerase (Applied Biosystems) in a 96-well thermocycler (GeneAmp 9700, Applied Biosystems) with the following cycle protocol: after 2 min at 94°C, 20 cycles (94°C, 30 s; 60°C, 30 s; 72°C, 35 s) of PCR were performed followed by a final elongation step of 5 min at 72 °C. Second-rounds PCR were performed using 10 µl of the first PCR product, and each marker was amplified individually using its specific primer pair by performing 35 PCR cycles (as described above) under similar conditions except that dNTPs concentration used was 200 µM.

The sequences of primer pairs (synthesized by Medicorp, Montreal, Qc, Canada) used were (from 5′ to 3′): ChAT (Brice et al., 1989): first-round PCR: sense, CAGGAAGGT CGGGTGGACAACATC (position 1564); antisense, TCCTTGGGTGCTGGTGGCTTG (position 2087); second-round PCR: sense, ATGGCCATTGACAACCATCTTCTG (position

1729); antisense, CCTTGAACTGCAGAGGTCTCTCAT (position 2052); GAD65 (accession number M72422): first and second-rounds PCR: sense, CCTTTCCT GGTGAGTGCCACAGCTGGAACC (position 1059); antisense, TTTGAGAGGCGGCT CATTCTCTCTTCATTG (position 1657); GAD67 (accession number M76177): first and second-rounds PCR: sense, TTTGGATATCATTGGTTTAGCTGGCGAAT (position 763); antisense, TTTTTGCCTCTAAATCAGCTGGAATTATCT (position 1163); VGLUT1 (accession number U07609): first and second-rounds PCR: sense, TACTGGAGAAGCGGCAGGAAGG (position 188); antisense, CCAGAAAAAGGAG CCATGTATGAGG (position 498); VGLUT2 (accession number AF271235): first and second-rounds PCR: sense, CCCGCAAAGCATCCAACCA (position 1264); antisense, TGAGAGTAGCCAACAACCAGAAGCA (position 1682).

Fifteen microliters of PCR products were run and visualized on 1.5% agarose gels stained with ethidium bromide, using a 100bp DNA ladder (Life Technologies) as molecular weight marker. The predicted sizes of the PCR products were (in bp) 324 (ChAT), 599 (GAD65), 401 (GAD67), 311 (VGLUT1) and 419 (VGLUT2).

Retrograde labeling of septohippocampal neurons. Young Sprague-Dawley rats (13-16 days old) were anesthetized with ketamine (75 mg/kg), xylazine (4 mg/kg) and acepromazine (0.075 mg/kg). Labeling of septohippocampal neurons was performed as described previously with minor modifications (Wu et al., 2000). Briefly, FITC-labelled latex microspheres (Lumafluor Inc., Naples, FL, USA) were infused bilaterally at 8 sites within the hippocampus (0.3 μl/site at a rate of 0.15 μl/min). The stereotaxic coordinates used for each site bilaterally were (in mm, relative to Bregma): (1) AP -2.8, L ±1.4, V -2.8; (2) AP -4, L ±1.8, V -2.8; (3) AP -5.5, L ±4.3,

V -4.5 and (4) AP -4, L ±1.8, V -3.5. Fluorescent latex microspheres have several advantages: they show little diffusion, are rapidly transported to the neuronal soma, the fluorescence persists for several weeks, and they are not cytotoxic (Katz et al., 1984; Katz and Iarovici, 1990). Rats were used at least 2 days later to prepare septal brain slices as described above for electrophysiological experiments. Injection sites in the hippocampus were controlled for each rat. FITC-labelled neurons were visualized using a confocal microscope (Bio-RAD microradiance, Hercules, CA, USA).

Pharmacological blockade of I_h. The bradycardic agent ZD7288 (4-(N-Ethyl-N-phenylamino)-1,2-dimethyl-6-(methylamino) pyridinium chloride) (Tocris Cookson, Ellisville, MO, USA), previously shown to act as a selective I_h current blocker in various CNS neurons (Gasparini and DiFranscesco, 1997; Khakh and Henderson., 1998; Larkham and Kelly, 2001; Lüthi et al., 1998; Maccaferi and McBain, 1996), was bath applied at a concentration of 100 μM. The current-clamp and voltage-clamp protocols described above were applied to each recorded neuron before and during perfusion with ZD7288.

Statistical analysis. All electrophysiological data were analyzed by an ANOVA followed by a Newman-Keuls test, otherwise stated, using Graphpad Prism (GraphPad Software, Inc., San Diego, CA, USA).

RESULTS

Chemical phenotype of electrophysiologically characterized medial septum - diagonal band complex neurons.

We investigated the electrophysiological properties of MSDB neurons and molecularly identified their chemical phenotype using sc-RT-PCR. Seventy-eight MSDB neurons were recorded and the expression of mRNAs encoding ChAT, GAD65, GAD67, VGLUT1 and VGLUT2 were then detected by multiplex single-cell RT-PCR. No correlation was noted between the phenotype and the location where it was recorded within the MSDB.

ChAT mRNA-positive neurons.

Fourteen of the 78 recorded neurons analysed by sc-RT-PCR were found to express ChAT but not GAD mRNAs. Figure 1 shows a typical example of the firing characteristics of a ChAT-positive neuron. This neuron expressed ChAT mRNA, but none of the other mRNAs investigated (Fig. 1A). However, it is noteworthy that 5 of the 14 ChAT-positive neurons also expressed one or both VGLUT mRNAs. Electrophysiologically, all ChAT-positive neurons appeared similar and exhibited firing properties of slow-firing neurons (Table 1), with a low and regular firing frequency in response to a threshold depolarizing current pulse applied from –60 or –80 mV (Fig. 1B,C). When depolarized from –80 mV, neuronal firing was usually delayed by a transient hyperpolarization of the membrane potential (Fig. 1C). Their mean firing rate (MF), maximal frequency (F_{MAX}) and steady frequency (F_{STEADY}) were low in comparison to the other groups (Table 1). Neurons in this population showed an important spike accommodation of 67.2 $\pm$ 34.1 %. Injection of hyperpolarizing current pulses induced a sustained hyperpolarization of

the membrane potential, with no obvious depolarizing sag at –95 mV (Table 1), and typically no rebound firing following the end of the hyperpolarizing current pulse (Fig. 1D). In voltage-clamp mode, series of hyperpolarizing voltage steps from –50 to –120 mV elicited an I_h current of relatively small amplitude and slow activation kinetic (Fig. 1E, F; Table 1).

GAD67 mRNA-positive neurons.

The second neuronal population comprised 24 cells that expressed GAD67 but not ChAT mRNAs. Of these, none expressed GAD65 mRNA, but half were found to coexpress mRNAs for the VGLUTs. Electrophysiologically, 12 of the 24 GAD67-positive neurons displayed characteristics typical of fast-firing neurons (Fig. 2A1-F1), with a relatively high sustained frequency of spike discharge in response to depolarizing current pulses applied from either -60 or -80 mV (Fig 2B1,C1). In this subpopulation, the MF, F_{MAX} and F_{STEADY} were higher than those found in ChAT-positive neurons (Table 1), but significantly lower than GAD67-positive, burst-firing neurons (see below). These neurons displayed a “sag” of intermediate amplitude between those found in slow-firing, ChAT-positive, and burst-firing GAD-positive neurons (Table 1), and was followed by a non-bursting rebound (Fig. 2D1). In voltage-clamp mode, these GAD67-positive, fast-firing neurons, had an I_h current (Fig. 2E1,F1) of significantly larger amplitude and of faster activation kinetic than those in ChAT-positive, slow-firing neurons (Table 1). The other 12 GAD67-positive neurons exhibited both fast- and burst-firing upon depolarization (burst-firing neurons; Fig. 2A2-F2). These neurons responded with a relatively high sustained firing frequency in response to a depolarizing current pulse applied from –60 mV (Fig. 2B2), but displayed burst firing in response to a depolarizing current pulse applied from –80 mV (Fig. 2C2). The MF, F_{MAX} and F_{STEADY} of this population were significantly higher than neurons from

all other groups (Table 1). These burst firing GAD67 mRNA-expressing neurons also typically displayed a prominent depolarizing sag in response to hyperpolarizing current pulse (Table 1) followed by burst rebound firing (Fig. 2D2). Neurons expressing solely GAD mRNAs accommodated less than those of the other populations with a value of 46.1 + 32.1 %. In voltage-clamp mode, the amplitude of I_h current in GAD67-positive, burst-firing neurons, was significantly larger than those in ChAT-positive, slow-firing neurons but not significantly different from GAD-67-positive fast- firing neurons (Fig. 2E2, F2; Table 1).

ChAT & GAD67 mRNAs-positive neurons.

A third neuronal population consisted of 19 neurons coexpressing both ChAT and GAD67 mRNAs. Amongst them, 15 also expressed mRNAs for the VGLUTs. This population of neurons was electrophysiologically heterogeneous but the large majority (16 of 19 cells) displayed fast-firing or burst-firing properties (Table 1). Figure 3 shows two examples of fast-firing and burst-firing ChAT & GAD67- positive neurons. Six of the 19 ChAT-GAD67-positive neurons were found to display electrophysiological properties similar to GAD67-positive, fast-firing neurons, with a rapid and sustained discharge in response to depolarizing current pulses applied from –60 or –80 mV (Fig. 3A1-F1). Their MF, F_{MAX} and F_{STEADY} were lower than ChAT & GAD67-positive, burst-firing neurons (see below), but higher than all slow-firing neurons. In these fast-firing neurons, hyperpolarizing current pulses elicited a slow activating depolarizing sag of moderate amplitude without bursting rebound firing (Fig. 3D1). The I_h current (Fig. 3E1-F1) was also of moderate amplitude (Table 1). Ten of the 19 ChAT & GAD67-positive neurons recorded exhibited electrophysiological properties similar to GAD67-positive, burst-firing neurons (Fig. 3A2-F2), with a fast firing from –60 mV (Fig 3B2), and burst firing from –80 mV (Fig 3C2).

Their MF, F_{MAX} and F_{STEADY} were relatively high and similar to those of GAD67-positive burst firing neurons. Neurons expressing ChAT&GAD had an accommodation value of 60.6 + 32.4 %. These neurons displayed a prominent depolarizing sag (Fig. 3D2; Table1), rebound firing characterized by a burst of action potentials (Fig. 3D2), and an I_h current of relatively large amplitude (Fig. 3E2,F2; Table 1). Finally, 3 ChAT & GAD67-positive neurons showed electrophysiological properties similar to those of ChAT-positive, slow-firing neurons (Table 1).

VGLUT mRNA-positive neurons.

We have identified a fourth neuronal population consisting of 21 neurons that expressed only VGLUT1 and/or VGLUT2 transcripts, without ChAT or GAD. Figure 4 shows the electrophysiological responses of a representative neuron coexpressing VGLUT1 and VGLUT2. Electrophysiologically, all recorded neurons in this group exhibited the properties of slow-firing neurons (Fig. 4B-F). Their MF, F_{MAX} and F_{STEADY} were similar to ChAT-positive, slow-firing neurons (Table 1). Overall, these neurons had an accommodation value of 75.0 + 33.1%. Interestingly, prolonged depolarizations revealed the occurrence of cluster firing in nearly half of these neurons that was separated by conspicuous subthreshold membrane oscillations (9/21 neurons, Fig. 4D, 5D and 6; Table 1). In contrast, similar depolarisations did not elicit cluster firing or subthreshold oscillations in ChAT and/or GAD expressing neurons. These neurons expressed a small depolarizing sag upon hyperpolarization, as well as a small I_h current, similar to those expressed by slow-firing, ChAT-positive neurons (Fig. 4D,E,F; Table 1).

Retrograde labelling of septohippocampal neurons.

We next wanted to determine if the different MSDB neuronal populations identified herein projected to the hippocampus, and thereby potentially contribute to hippocampal activity. Injection of fluorescent latex microspheres at several sites within the hippocampus at least 2 days prior to recording allowed labelling of a relatively high number of cell bodies in the MSDB. Of the 33 MSDB FITC-labelled neurons, 24 were found to exhibit the firing properties of slow-firing, ChAT-positive neurons, with a slow and regular activity in response to depolarizing current pulses, often delayed by a transient hyperpolarization, and no depolarizing sag in response to hyperpolarizing current pulses (Fig. 5A). Another group of retrogradely-labelled neurons (5 of 33 neurons) had firing properties similar to fast-firing GAD67-positive or ChAT & GAD67-positive neurons, with a fast and regular firing activity in response to depolarizing current pulses and a depolarizing sag in response to hyperpolarizing current pulses (Fig. 5B). Three of these retrogradely-labelled neurons also exhibited firing properties of burst-firing neurons (Fig. 5C), with a prominent depolarizing sag in response to hyperpolarizing current pulses, and rebound firing characterized by a burst of action potentials, similar to burst-firing GAD67-positive, or ChAT-GAD67-positive neurons. Finally, 4 retrogradely labelled neurons responded to depolarizing steps with cluster-firing and subthreshold oscillations similar to neurons expressing solely VGLUT1and/or VGLUT2 mRNAs (Fig. 5D). We further investigated the voltage-sensitivity of the oscillations displayed by VGLUT-positive neurons (Fig. 6). Both the frequency of action potentials within the clusters, and the subthreshold membrane oscillations occurring between clusters, were similarly voltage-dependent, and increased in frequency near 20-25 Hz for depolarisations up to –47 mV (Fig. 6B,C). The frequency of the

inter-clusters was slightly voltage-sensitive, increasing from 0 to 2 Hz upon depolarization (Fig. 6D).

Effects of selective I_h blockade by ZD7288 on firing properties of MSDB neurons.

The I_h current serves as a pacemaker in many neuronal cell types in the brain and may also be implicated in septohippocampal rhythm generation (Xu et al., 2002). We therefore investigated the role of I_h in MSDB neurons using ZD7288, a pharmacological agent reported to be a selective blocker of I_h current in neurons (Khakh and Henderson, 1998; Maccaferi and McBain, 1996; Gasparini and DiFranscesco, 1997; Larkham and Kelly, 2001; Lüthi et al., 1998).

Although an I_h current has been previously observed in non-cholinergic neurons (Griffith, 1998; Garoleva and Reiner, 1996), it remains unclear what the role of I_h is on the firing frequency and burst firing in the different MSDB population. In 5 fast-firing neurons, bath application of 100 μM ZD7288 induced a complete and irreversible blockade of the inward current evoked by hyperpolarizing voltage steps (Fig. 7A), and the depolarizing sag induced by hyperpolarizing current pulses (Fig. 7B). ZD7288 also caused a more than two-fold increase in the delay of rebound-firing occurring following the end of the hyperpolarizing current pulse (from 102.3 ± 54.6 ms to 268.9 ± 256.3 ms; ZD7288/control = 234 ± 83 %; Fig. 7B & 8B) and decreased by nearly half the instantaneous frequency of rebound firing (from 17.4 ± 3.6 to 10.3 ± 3.2 Hz; ZD72288/control = 55 ± 25 %; Fig. 7B & 8C). The mean firing rate of fast-firing neurons in response to depolarizing current pulses applied from –80 mV was also decreased by ZD7288 (from 9.8 ± 2.3 to 5.0 ± 1.6 Hz; Fig. 7B & 8A), whereas it was not affected in response to depolarizing current pulses applied from –60 mV (not shown).

In 5 burst-firing neurons, bath application of 100 μM ZD7288 also induced a complete and irreversible blockade of I_h current (Fig. 7C), and the depolarizing sag induced by hyperpolarizing

current pulses (Fig. 7D). I_h current blockade produced a three-fold increase in the delay of rebound firing (from 44.5 ± 7.3 to 149.5 ± 28.4 ms; ZD7288/control = 377 ± 123 %; Fig. 7D & 8B) and a pronounced decrease in the instantaneous frequency within the burst (from 140.9 ± 41.2 to 50.9 ± 27.6 Hz; ZD7288/control = 40 ± 13 %; Fig. 7D & 8C). The mean firing rate of burst-firing neurons when depolarized from –80 mV was also strongly decreased by ZD7288 (from 18.2 ± 7.4 to 8.6 ± 3.1 Hz; Fig. 7D & 8A) whereas the frequency was not affected when depolarized from –60 mV (not shown).

In 8 slow-firing and cluster-firing neurons, the small I_h current and depolarizing sag were blocked by bath application of ZD7288 (Fig. 7E, G). In contrast to the results from the two other neuronal populations, ZD7288 did not affect the mean firing frequency of slow-firing and cluster-firing neurons (Fig. 7F, H). All results for the effects of ZD7288 on the mean frequency, rebound firing delay and the rebound instantaneous frequency are summarized in Fig. 8A, B and C, respectively. The antagonist ZD7288 did not appear to reduce cluster firing or subthreshold oscillations, suggesting that these oscillations are mediated by other conductances. We next determined the correlation between firing frequency and I_h magnitude. As expected, a high positive linear relationship was found between the amplitude of I_h (determined in voltage-clamp mode) and the depolarizing sag (recorded in current-clamp mode) for the slow-firing (n=30), fast-firing (n=17) and burst-firing (n=17) neurons (correlation coefficient, R^2=0.9726; Fig. 8D). Interestingly, we also found a very high linear relationship between the mean firing rate in each of the 3 groups and the amplitude of the depolarizing sag (correlation coefficient, R^2=0.9968; Fig. 8E) or I_h amplitude (correlation coefficient, R2=0.9879; Fig 8F), suggesting that I_h contributes to firing frequency.

DISCUSSION

Septohippocampal non-cholinergic neurons play a key pacemaker role for hippocampal rhythmical activity. Eventhough non-cholinergic neurons have been intensively investigated in the past, their chemical identity still remains largely unknown. Using an approach that combines electrophysiology to single-cell RT-PCR, we report that the MSDB contains GABAergic neurons displaying fast-firing activity, often associated with burst-firing involving in part I_h current. Moreover, we show for the first time that an important proportion of MSDB neurons is putatively glutamatergic. These glutamatergic neurons display unique firing behavior characterized by cluster-firing with underlying voltage-dependent subthreshold membrane oscillations. Our data suggest that MSDB bursting GABAergic and cluster-firing glutamatergic neurons, since they provide projections to the hippocampus, may contribute distinct pacemaker activity to the hippocampal rhythm.

Chemical phenotype of electrophysiologically characterized MSDB neurons

The first part of our results showed that neurons expressing ChAT mRNA exhibited electrophysiological properties of slow-firing neurons, lacking any I_h current and that neurons with such properties projected to the hippocampus. This neuronal population is similar to slow-firing neurons previously identified immunohistochemically as cholinergic (Alreja et al., 2000; Gorelova and Reiner, 1996; Griffith and Matthews, 1986; Markam and Segal, 1990). Unlike cholinergic neurons of the more caudally located basal forebrain (Khateb et al., 1992), MSDB cholinergic neurons did not show low-threshold bursts.

We found a second neuronal population that is likely GABAergic. Previous studies have failed to determine which electrophysiologically recorded MSDB population were GABAergic since

performing GABA or GAD immunocytochemistry on recorded neurons has been extremely difficult (Knapp et al., 2000). Nevertheless, previous studies have suggested that a subpopulation of fast-firing neurons may be GABAergic (Knapp et al., 2000; Morris et al., 1999), but the phenotype of neurons displaying burst firing has not yet been determined (Knapp et al., 2000; Morris et al., 1999; Morris and Henderson, 1999). Our results demonstrate for the first time that all neurons exhibiting either fast-firing, or a combination of fast- and burst-firing, expressed GAD67 mRNA, providing strong evidence that they are GABAergic. Another group (24%) was found to coexpress ChAT and GAD67 mRNAs. Recent studies using acutely dissociated MSDB or basal forebrain neurons also found similar proportions of neurons (approximately 25%) coexpressing ChAT and GAD67 mRNAs (Han et al., 2002; Puma et al., 2001; Tkatch et al., 1998). Most neurons in this population were electrophysiologically very similar to the group expressing solely GAD67 mRNAs without ChAT, because they displayed either fast-firing, or both fast- and burst-firing and exhibited a significant I_h. These neurons are likely GABAergic, and not cholinergic, since by exclusion, no fast-firing or burst-firing neurons were ever shown to stain with ACh immunohistochemical markers (Alreja et al., 2000; Gorelova and Reiner, 1996; Griffith and Matthews, 1986; Markam and Segal, 1990). Moreover, combined immunohistochemical staining for ChAT and GAD revealed only a few (1%) double-labelled cells in the MSDB (Brashear et al., 1986; Gritti et al., 1993; Kosaka et al., 1988), suggesting that ChAT and GAD coexpression may be a rare occurrence. Taking together previous results and those from the present study, we suggest that these neurons may normally release GABA but since they have both synthesizing enzymes, they may also have the capability to synthesize and release acetylcholine in certain circumstances that need to be determined. Our results also provide evidence that putative GABAergic MSDB neurons displaying fast-firing, or both fast-

and burst-firing, were probably hippocampal projecting neurons. This is in agreement with previous results showing that fast-firing and burst-firing MSDB neurons are antidromically activated following fornix stimulation (Henderson et al., 2001; Jones et al., 1999), and that some medial septum fast-firing neurons are labelled following injection of retrograde marker into the hippocampus (Wu et al., 2000). Based on the results combining single-cell RT-PCR and electrophysiology, it is likely that the septohippocampal neurons diplaying fast- and burst-firing, in this and other studies, were GABAergic.

I_h current contributes to burst firing in GABAergic neurons

The I_h current is a key ionic conductance implicated in generating rhythmic bursts in a number of brain structures such as thalamus, hippocampus and cortex (Dickson et al., 2000; Lüthi et al., 1998; Lüthi and McCormick, 1998; Maccaferri and McBain, 1996). Acting in concert with the low-threshold calcium current, the I_h current in MSDB neurons may also be critical in generating bursts necessary for driving hippocampal rhythmical activity. Recent preliminary evidence supports this proposal since I_h current blockade in the MSDB blocks hippocampal theta rhythmicity (Xu et al., 2002). One key finding in this study is that MSDB GABAergic neurons, but not cholinergic or glutamatergic neurons, have the capacity to emit bursts of action potentials, which initiation and frequency seem to be partly dependent on the activation of I_h current. The presence of burst-firing only in GAD mRNA-positive neurons supports previous suggestions that MSDB GABAergic bursting neurons are implicated in hippocampal pacemaker activity (Stewart and Fox, 1989, 1990; King et al., 1998). However, the mechanism involved in generating regenerative pacemaker activity of GABAergic MSDB neurons remains unknown since sustained rhythmic bursting in these neurons was not observed in our slice preparation.

This indicates that rhythmic bursting activity of MSDB GABAergic neurons may necessitate one or a combination of neurotransmitters such as acetylcholine and serotonin (Colom and Bland, 1991; Stewart and Fox, 1989), a pacemaker input onto the GABAergic septal neurons, such as supramammillary nucleus (Vertes and Kocsis, 1997), or connections from the hippocamposeptal feedback inhibitory loop (Wang, 2002).

The MSDB may contain septohippocampal glutamatergic neurons

The MSDB has traditionally been thought to contain only cholinergic and GABAergic neurons (Stewart and Fox, 1990). Surprisingly, we found an additional neuronal population that did not express transcripts for ChAT or GAD65/67, but that expressed one or both vesicular glutamate transporters. The vesicular glutamate transporters 1 & 2 are believed to be markers for glutamate releasing neurons (Fremeau et al., 2001; Fujiyama et al, 2001; Herzog et al., 2001; Takamori et al., 2001) strongly suggesting that the MSDB contains a neuronal population that is likely glutamatergic. Moreover, single-cell RT-PCR performed on more than 100 randomly picked whole neurons from acutely dissociated MSDB also revealed a high number of ChAT-negative, GAD-negative and VGLUT-positive neurons (Danik M, Manseau F, Sotty F, Quirion R, Williams S, Unpublished observations). Our results are in agreement with recent immunohistochemical studies showing that the MSDB contains a subset of phosphate-activated glutaminase (PAG)-positive neurons (an enzyme involved in neuronal glutamate synthesis) but that are GAD- and ChAT-negative (Manns et al., 2001). Recently, Kiss et al., (2002) also showed that some MSDB neurons projecting to the supramammilary nucleus may operate with aspartate or glutamate. Furthermore, electrophysiological studies in septohippocampal co-cultures have shown that stimulation of the medial septum produced fast excitatory post-synaptic

currents mediated by glutamate in post-synaptic hippocampal cells (Gahwiler and Brown, 1985), strongly suggesting the existence of glutamatergic transmission in the septohippocampal pathway. A unique characteristic of MSDB VGLUT1/2 mRNA expressing neurons is their capacity to discharge in recurrent clusters of action potentials, interspersed with intrinsically generated subthreshold membrane potential oscillations. The unique firing features of these neurons are unlikely to be due to the patch recording method per se since they were only observed in VGLUT-positive neurons. Both the intracluster and the subthreshold oscillations frequencies were similarly voltage-dependent and increased up to 25 Hz at –47 mV, whereas the intercluster frequency remained inferior to 2 Hz. Cluster-firing MSDB neurons have been described previously (Serafin et al., 1996), but the mean maximum frequency of intraclusters (37 Hz), subthreshold oscillations (40 Hz) and interclusters (4 Hz) were faster than those reported here (25, 25 and 2 Hz, respectively) and they also expressed a notable I_h. These differences could be due in part to different experimental conditions (ie temperature, recording technique, age of animals). These cluster-firing, putative glutamatergic septohippocampal neurons, are likely to modulate hippocampal activity and may also contribute to the recently reported glutamate generated theta-like rhythm in hippocampal pyramidal neurons (Bonansco and Bruno, 2003). These cluster-firing neurons may also be similar to the extracellularly recorded basal forebrain PAG-immunopositive, ChAT- and GAD-immunonegative neurons, shown to fire rhythmically in association with theta-like activity during cortical activity (Manns et al., 2003).

An intriguing finding in the present study was the widespread coexpression of VGLUT1 and/or 2 mRNAs with GAD or ChAT mRNAs in MSDB neurons. The extensive expression of VGLUT1 and 2 mRNAs suggest that many MSDB neurons have the biochemical machinery necessary for vesicular glutamate transport and release. An important expression of VGLUT transcript and

protein has been recently observed in the medial septum (Lin et al., 2003). This important expression of glutamate markers in the MSDB is consistent with immunohistochemical data demonstrating that a proportion of MSDB neurons that expressed PAG also had GAD or ChAT (Manns et al., 2001). Whether glutamate can be coreleased with acetylcholine or GABA from MSDB neurons remains to be explored. Co-release of GABA and glutamate, or GABA and acetylcholine, may be a possibility since it has been observed in other structures such as hippocampal granular neurons (Walker et al., 2000) and retinal cells (Santos et al.,1998), respectively.

Implication of the findings

The notion that GABAergic and cholinergic MSDB neurons play key roles in hippocampal rhythmicity, particularly activity in the theta frequency, has dominated the "septohippocampal field" for more than two decades. Our data suggest that only GABAergic septohippocampal neurons are endowed with bursting capability. These results support the hypothesis that septohippocampal GABAergic neurons, by firing in rhythmical bursts, may help pace GABAergic hippocampal interneurons and contribute to hippocampal oscillations (Freund et al., 1988; Cobb et al., 1995; Toth et al., 1997). Although MSDB bursting GABAergic neurons are unlikely to pace cholinergic and hippocampal inhibitory neurons by themselves, they may however be able to accurately transfer rhythmic burst discharges coming from other structures to these follower neurons. Our novel finding of septohippocampal glutamatergic neurons may also have important implications in learning and memory. These glutamate neurons are endowed with subthreshold oscillations and may therefore contribute to rhythm generation in hippocampus, events important for plasticity. Moreover, glutamate induced excitotoxicity originating from

MSDB neurons may also contribute to the well-established vulnerability of the MSDB in Alzheimer's disease.

REFERENCES

Alreja M, Wu M, Liu W, Atkins JB, Leranth C, Shanabrough M (2000) Muscarinic tone sustains impulse flow in the septohippocampal GABA but not cholinergic pathway: implications for learning and memory. J Neurosci 20:8103-8110.

Apartis E, Poindessous-Jazat FR, Lamour YA & Bassant MH (1998) Loss of rhythmically bursting neurons in rat medial septum following selective lesion of septo-hippocampal cholinergic system. J Neurophysiol 79, 1633-1642.

Bland BH & Oddie SD (2001) Theta band oscillation and synchrony in the hippocampal formation and associated structures: the case for its role in sensorimotor integration. Behav Brain Res 127,119-136.

Bonansco, C. & Buno, W. (2003). Cellular mechanisms underlying the rhythmic bursts induced by NMDA microiontophoresis at the apical dendrites of CA1 pyramidal neurons. *Hippocampus* **13**, 150-163.

Brashear HR, Zaborsky L & Heimer L (1986) Distribution of GABAergic and cholinergic neurons in the rat diagonal band. Neuroscience 17,439-451.

Brazhnik ES & Fox SE (1997) Intracellular recordings from medial septal neurons during hippocampal theta rhythm. Exp Brain Res 114,442-453.

Brice A, Berrard S, Raynaud S, Ansiaeu S, Coppola T, Weber MJ & Mallet J (1989) Complete sequence of a cDNA encoding an active rat choline acetyltransferase: a tool to investigate the plasticity of cholinergic phenotype expression. J Neurosci Res 23,266-273.

Buzsaki G (2002) Theta oscillations in the hippocampus. Neuron 33,325-340.

Cobb SR, Buhl EH, Halasy K, Paulsen O & Somogyi P (1995) Synchronisation of neuronal activity in hippocampus by individual GABAergic interneurons. Nature, 378:75-78.

Colom, L. V. & Bland, B. H. (1991). Medial septal cell interactions in relation to hippocampal field activity and the effects of atropine. *Hippocampus* **1**, 15-30.

Dickson CT, Magistretti J, Shalinsky MH, Fransen E, Hasselmo ME & Alonso A (2000) Properties and role of Ih in the pacing of subthreshold oscillations in entorhinal cortex layer II neurons. J Neurophysiol 83,2562-2579.

Fremeau RT Jr, Troyer MD, Pahner I, Nygaard GO, Tran CH, Reimer RJ, Bellocchio EE, Fortin D, Storm-Mathisen J & Edwards RH (2001) The expression of vesicular glutamate transporters defines two classes of excitatory synapse. Neuron 31,247-260.

Freund TF (1989) GABAergic septohippocampal neurons contain parvalbumin. Brain Res 478,375-381.

Freund TF & Antal M (1988) GABA-containing neurons in the septum control inhibitory interneurons in the hippocampus. Nature 336,170-173.

Fujiyama F, Furuta T & Kaneko T (2001) Immunocytochemical localization of candidates for vesicular glutamate transporters in the rat cerebral cortex. J Comp Neurol 435,379-387.

Gahwiler BH & Brown DA (1985) Functionnal innervation of cultured hippocampal neurons by cholinergic afferents from co-cultured septal explants. Nature 313,577-579.

Gasparini S & DiFranscesco D (1997) Action of the hyperpolarization-activated current (Ih) blocker ZD 7288 in hippocampal CA1 neurons. Pflügers Arch 435,99-106.

Gorelova N & Reiner PB (1996) Role of the afterhyperpolarization in control of discharge properties of septal cholinergic neurons in vitro. J Neurophysiol 75,695-706.

Griffith WH (1988) Membrane properties of cell types within guinea pig basal forebrain nuclei in vitro. J Neurophysiol 59,1590-1612.

Griffith WH & Matthews RT (1986) Electrophysiology of AChE-positive neurons in basal forebrain slices. Neurosci Lett 71,169-174.

Gritti I, Mainville L & Jones BE (1993) Codistribution of GABA- with acetylcholine-synthetizing neurons in the basal forebrain of the rat. J Comp Neurol 329,438-457.

Gritti I, Mainville L, Mancia M & Jones BE (1997) GABAergic and other noncholinergic basal forebrain neurons, together with cholinergic neurons, project to the mesocortex and isocortex in the rat. J Comp Neurol 383,163-177.

Gritti I, Manns ID, Mainville L, Jones BE (2003) Parvalbumin, calbindin, or calretinin in cortically projecting and GABAergic, cholinergic, or glutamatergic basal forebrain neurons of the rat. J Comp Neurol 458: 11-31.

Han S-H, McCool BA, Murchison D, Nahm S-S, Parrish A & Griffith WH (2002) Single-cell RT-PCR detects shifts in mRNA expression profiles of basal forebrain neurons during aging. Mol Brain Res 98,67-80.

Henderson Z, Morris NP, Grimwood P, Fiddler G, Yang HW & Appenteng K (2001) Morphology of local axon collaterals of electrophysiologically characterised neurons in the rat medial septal/ diagonal band complex. J Comp Neurol 430,410-432.

Herzog E, Bellenchi GC, Gras C, Bernard V, Ravassard P, Bedet C, Gasnier B, Giros B & El Mestikawy S (2001) The existence of a second vesicular glutamate transporter specifies subpopulations of glutamatergic neurons. J Neurosci 21,RC181(1-6).

Jones GA, Norris SK & Henderson Z (1999) Conduction velocities and membrane properties of different classes of rat septo-hippocampal neurons recorded *in vitro*. J Physiol (Lond) 517,867-877.

Khateb A, Muhlethaler M, Alonso A, Serafin M, Mainville L, Jones BE (1992) Cholinergic nucleus basalis neurons display the capacity for rhythmic bursting activity mediated by low-threshold calcium spikes. Neuroscience 51: 489-494.

Katz LC, Burkhalter A & Dreyer W (1984) Fluorescent latex microspheres as a retrograde neuronal marker for in vivo and in vitro studies of visual cortex. Nature 310, 498-500.

Katz LC & Iarovici DM (1990) Green fluorescent latex microspheres: a new retrograde tracer. Neuroscience 34,511-520.

Katz, L. C. & Iarovici, D. M. (1990). Green fluorescent latex microspheres: a new retrograde tracer. *Neuroscience* **34**, 511-520.

King C, Recce M & O'Keefe J. (1998) The rhythmicity of cells of the medial septum/diagonal band of Broca in the awake freely moving rat: relationships with behaviour and hippocampal theta. Eur J Neurosci 10,464-477.

Kiss J, Csáki Á, Bokor H, Kocsis K & Kocsis B (2002) Possible glutamatergic/aspartatergic projections to the supramammillary nucleus and their origins in the rat studied by selective [^{3}H]D-aspartate labelling and immunocytochemistry. Neuroscience 111,671-691.

Khakh BS & Henderson G (1998) Hyperpolarization-activated cationic current (Ih) in neurons of the trigeminal mesencephalic nucleus of the rat. J Physiol (Lond) 510,695-704.

Knapp JA, Morris NP, Henderson Z & Matthews RT (2000) Electrophysiological characteristics of non-bursting, glutamate decarboxylase messenger RNA-positive neurons of the medial septum/diagonal band nuclei of guinea-pig and rat. Neuroscience 98,661-668.

Kosaka T, Tauchi M & Dahl JL (1988) Cholinergic neurons containing GABA-like and/or glutamic acid decarboxylase-like immunoreactivities in various brain regions of the rat. Exp Brain Res 70,605-617.

Larkman PM & Kelly JS (2001) Modulation of the hyperpolarisation-activated current, Ih, in rat facial motoneurones in vitro by ZD-7288. Neuropharmacology 40,1058-1072.

Lee MG, Chrobak JJ, Sik A, Wiley RG & Buzsáki G (1994) Hippocampal theta activity following selective lesion of the septal cholinergic system. Neuroscience 62,1033-1047.

Lin W, McKinney K, Liu L, Lakhlani S & Jennes L (2003) Distribution of vesicular glutamate transporter-2 messenger ribonucleic Acid and protein in the septum-hypothalamus of the rat. Endocrinology:144,662-70.

Lüthi A, Bal T & McCormick DA (1998) Periodicity of thalamic spindle waves is abolished by ZD7288, a blocker of Ih. J Neurophysiol 79,3284-3289.

Lüthi A & McCormick DA (1998) H-current: properties of a neuronal and network pacemaker. Neuron 21,9-12.

Maccaferri G & McBain CJ (1996) The hyperpolarization-activated current (Ih) and its contribution to pacemaker activity in rat CA1 hippocampal stratum oriens-alveus interneurones. J Physiol (Lond) 497,119-130.

Manns ID, Alonso A & Jones BE (2000) Rhythmic discharge of identified cholinergic, GABAergic and glutamatergic juxtacellularly labelled and immunohistochemically identified basal forebrain neurons in relation to EEG activity. Soc Neurosci Abstr 26,1514.

Manns ID, Mainville L & Jones BE (2001) Evidence for glutamate, in addition to acetylcholine and GABA, neurotransmitter synthesis in basal forebrain neurons projecting to the entorhinal cortex. Neuroscience 107,249-263.

Manns, I. D., Alonso, A., & Jones, B. E. (2003). Rhythmically discharging basal forebrain units comprise cholinergic, GABAergic, and putative glutamatergic cells. *J.Neurophysiol.* **89**, 1057-1066.

Markram H & Segal M (1990) Electrophysiological characterization of cholinergic and non-cholinergic neurons in the rat medial septum/diagonal band complex. Brain Res 513,171-174.

Morris NP, Harris SJ & Henderson Z (1999) Parvalbumin-immunoreactive, fast-spiking neurons in the medial septum/diagonal band complex of the rat: intracellular recordings *in vitro*. Neuroscience 92,589-600.

Morris NP & Henderson Z (2000) Perineuronal nets ensheath fast spiking, parvalbumin-immunoreactive neurons in the medial septum/diagonal band complex. Eur J Neurosci 12,828-838.

Pape H (1996) Queer current and pacemaker: the hyperpolarization-activated cation current in neurons. Ann Rev Physiol 58,299-327.

Puma C, Danik M, Quirion R, Ramon F & Williams S (2001) The chemokine interleukin-8 acutely reduces Ca(2+) currents in identified cholinergic septal neurons expressing CXCR1 and CXCR2 receptor mRNAs. J Neurochem 78,960-971.

Ruano D, Lambolez B, Rossier J, Paternain AV & Lerma J (1995) Kainate receptor subunits expressed in single cultured hippocampal neurons: molecular and functional variants by RNA editing. Neuron 14,1009-1017.

Santos PF, Carvalho A.L, Carvalho AP & Duarte CB (1998) Differential acetylcholine and GABA release from cultured chick retina cells. Eur. J. Neurosci 10**,** 2723-2730.

Serafin M, Williams S, Khateb A, Fort P & Mühlethaler M (1996) Rhythmic firing of medial septum non-cholinergic neurons. Neuroscience 75,671-675.

Stewart M & Fox SE (1989) Detection of an atropine-resistant component of the hippocampal theta rhythm in urethane-anesthetized rats. Brain Res 500,55-60.

Stewart M & Fox SE (1990) Do septal neurons pace the hippocampal theta rhythm? TINS 13,163-168.

Takamori S, Rhee JS, Rosenmund C & Jahn R (2001) Identification of differentiation-associated brain-specific phosphate transporter as a second vesicular glutamate transporter (VGLUT2). J Neurosci 21,RC182(1-6).

Thoby-Brisson, M., Telgkamp, P., & Ramirez, J. M. (2000). The role of the hyperpolarization-activated current in modulating rhythmic activity in the isolated respiratory network of mice. *J.Neurosci*. **20**, 2994-3005.

Tkatch T, Baranauskas G & Surmeier DJ (1998) Basal forebrain neurons adjacent to the globus pallidus co-express GABAergic and cholinergic marker mRNAs. Neuroreport 9,1935-1939.

Tóth K, Freund TF & Miles R (1997) Disinhibition of rat hippocampal pyramidal cells by GABAergic afferents from the septum. J Physiol (Lond) 500,463-474.

Vertes RP& Kocsis B (1997) Brainstem-diencephalo-septohippocampal systems controlling the theta rhythm of the hippocampus. Neuroscience 81,893-926.

Walker MC, Ruiz A & Kullmann DM (2000) Monosynaptic GABAergic signaling from dentate to CA3 with a pharmacological and physiological profile typical of mossy fiber synapses. Neuron 29,703-15.

Wang XJ (2002) Pacemaker neurons for the theta rhythm and their synchronization in the septohippocampal reciprocal loop. J Neurophysiol 87:889-900.

Wu M, Shanabrough M, Leranth C, Alreja M (2000) Cholinergic excitation of septohippocampal GABA but not cholinergic neurons: Implications for learning and memory. Journal of Neuroscience 20: 3900-3908.

Xu C, Datta S, Wu M & Alreja M (2002) Suppression of the H-current in septohippocampal GABAergic neurons blocks hippocampal theta rhythm. Program No. 430.5. *2002 Abstract Viewer/Itinerary Planner*. Washington, DC: Society for Neuroscience, 2002.

Figure 1. ChAT-positive neurons display electrophysiological properties of slow-firing neurons. A, Agarose gel analysis of the RT-mPCR products obtained from a single MSDB cell. The only PCR-generated fragment was that of ChAT. B, C, Current-clamp recordings in the same MSDB neuron of the membrane responses to injection of depolarizing current pulses applied from a membrane potential of –60 mV (B) or –80 mV (C). This neuron displays a slow and regular firing activity. D, Response recorded in current-clamp mode to injection of a hyperpolarizing current pulse from –60 mV. Note the absence of depolarizing sag in response to membrane hyperpolarization, and of rebound firing when returning to –60 mV. E, Currents recorded in voltage-clamp mode evoked by a series of hyperpolarizing voltage steps applied from a holding potential of –50 mV. Notice the small amplitude inward current in this cell, as shown by the difference between the amplitudes of the instantaneous current (open circle) and steady-state current (closed circle). F, Instantaneous and steady-state I-V plots derived from the data in E. (B, C, D: vertical bars: 20 mV; horizontal bars: 200 ms).

Figure 2. GAD67-positive neurons display electrophysiological properties of either burst-firing or fast-firing neurons. A1-F1 (left panel): Example of a GAD-positive, fast-firing neuron. This particular neuron expressed only GAD67 mRNA (A1). This neuron displayed a fast and regular firing activity when depolarized from both –60 mV (B1) and –80 mV (C1). Injection of hyperpolarizing current pulses in this neuron induced a moderate depolarizing sag (D1). Rebound firing was weak without bursts (D1). Voltage-clamp recordings of currents evoked by a series of hyperpolarizing voltage steps applied from a holding potential of –50 mV show the presence of a moderate inward current in this cell (E1), indicated by a difference in amplitude between the instantaneous current (open circle) and steady-state current (closed circle). F1,

Instantaneous and steady-state I-V plots derived from the data in E1. A2-F2 (right panel): Example of a GAD-positive, burst-firing neuron. Agarose gel analysis of the RT-mPCR products obtained from a single MSDB cells shows that this particular neuron expressed only GAD67 mRNA (A2). This neuron displayed a fast and regular firing activity when depolarized from –60 mV (B2), and burst firing when depolarized from –80 mV (C2). Burst firing was characterized by few action potentials riding on a slow depolarizing wave (inset C2). Injection of hyperpolarizing current pulses in this neuron induced a profound depolarizing sag (D2). Rebound firing appeared as a burst of action potentials (inset D2). E2: Voltage-clamp recordings of currents elicited by a series of hyperpolarizing voltage steps applied from a holding potential of –50 mV. Note the presence of a rapidly activating and large inward current in this cell, as shown by the difference between the amplitude of the instantaneous current (open circle) and steady-state current (closed circle). F2, Instantaneous and steady-state I-V plots derived from the data in E2. (B, C, D: vertical bars: 20 mV; horizontal bars: 200 ms).

Figure 3. Most ChAT & GAD67- positive neurons display electrophysiological properties of either burst-firing or fast-firing neurons. A1-F1: Example of a ChAT & GAD-positive, fast-firing neuron. This particular neuron expressed ChAT & GAD67 mRNAs (A1). In current-clamp mode, this neuron displayed a fast and regular firing activity when depolarized from both –60 mV (B1) and –80 mV (C1). Injection of a hyperpolarizing current pulse in this neuron induced a moderate depolarizing sag (D1). Rebound firing appeared as a single action potential (D1). E1: Voltage-clamp recordings of currents evoked by a series of hyperpolarizing voltage steps applied from a holding potential of –50 mV show the presence of a moderate inward current in this cell, corresponding to the difference between the amplitude of the instantaneous current (open circle)

and steady-state current (closed circle). F1: Instantaneous and steady-state I-V plots derived from the data in E1. A2-F2: Example of a ChAT & GAD-positive, burst-firing neuron. Agarose gel analysis of the RT-mPCR products obtained from a single MSDB cells shows that this particular neuron expressed both ChAT and GAD67 mRNAs, as well as VGLUT1 and VGLUT2 mRNAs (A2). This neuron displayed a fast and regular firing activity when depolarized from–60 mV (B2), and burst firing when depolarized from –80 mV (C2). Injection of hyperpolarizing current pulses in this neuron induced a fast and large depolarizing sag (D2). Rebound firing appeared as a burst of action potentials (D2). Voltage-clamp recordings of currents evoked by a series of hyperpolarizing voltage steps applied from a holding potential of –50 mV showing the presence of a fast and large inward current in this cell (E2), as shown by the difference between the amplitude of the instantaneous current (open circle) and steady-state current (closed circle). F2: Instantaneous and steady-state I-V plots derived from the data in E2. (B, C, D: vertical bars: 20 mV; horizontal bars: 200 ms).

Figure 4. VGLUT-positive neurons display electrophysiological properties of cluster-firing neurons. A, Agarose gel analysis of the RT-mPCR products obtained from a single MSDB cell showing the coexpression of both VGLUT1 and VGLUT2 mRNAs. B, C, Current-clamp recordings in the same MSDB neuron of the membrane responses to injection of depolarizing current pulses applied from a membrane potential of –60 mV (B) or –80 mV (C). This neuron displayed a slow firing activity when depolarized from both membrane potentials. D, Depolarizations up to –45 mV elicited cluster firing and subthreshold membrane oscillations between clusters. E, Current-clamp recordings of the membrane response to injection of a hyperpolarizing current pulse from –60 mV. Note the absence of depolarizing sag in response to

membrane hyperpolarization, and the absence of rebound firing when returning to –60 mV. F, Voltage-clamp recordings of currents evoked by a series of hyperpolarizing voltage steps applied from a holding potential of –50 mV. Note the absence of inward current in this cell, as shown by the difference between the amplitude of the instantaneous current (open circle) and steady-state current (closed circle). G, Instantaneous and steady-state I-V plots derived from the data in E. (B, C, D: vertical bars: 20 mV; horizontal bars: 200 ms).

Figure 5. Slow-firing, fast-firing, burst-firing and cluster-firing neurons project to the hippocampus. Septohippocampal neurons were labelled by prior injection of fluorescent latex microspheres at several sites within the hippocampus. A1-D1: FITC-labelled neurons were vizualized in MSDB slices by confocal imaging (left images), and the overlay of both fluorescence and transmission images showing the patch pipette (right images). Electrophysiological recordings in current-clamp mode are shown for slow-firing (A2-A4), fast-firing (B2-B4), burst-firing (C2-C4) and cluster-firing (D2-D4) retrogradely labelled neurons. Neuronal response to injection of depolarizing current pulses applied from –60 mV (A2-D2) or –80 mV (A3-D3), as well as to injection of hyperpolarizing current pulses applied from –60 mV (A4-D4) are shown. (B, C, D: vertical bars: 20 mV; horizontal bars: 200 ms).

Figure 6. Intracluster, intercluster and subthreshold oscillations frequencies in VGLUT-positive, septohippocampal cluster-firing neurons, are voltage-dependent. A**,** FITC-labelled septohippocampal neuron is shown with a patch pipette. B, this neuron recorded in current-clamp mode showed cluster-firing in response to injection of depolarizing current pulses of increasing amplitude. An enlargement of subthreshold oscillations is shown on the right (a-c) for each trace

depicted to the left. The frequency of the membrane oscillations increased with depolarized membrane potentials (-54 to –47 mV). In this cluster-firing neuron, the frequency of subthreshold oscillations was near 25 Hz at –47 mV (oscillations indicate by dots are shown enlarged on the right panel), and decreased to about 10 Hz at –54 mV. At –50 mV, the intracluster, intercluster and subthreshold oscillations frequencies were lower than at –47 mV. The enlargement on the right panel (b) shows the subthreshold oscillations emerging and preceding firing of action potentials (arrows). At –54 mV, the intraclusters and interclusters frequencies were very low but subthreshold oscillations were still present (right panel). C, histograms showing that the intracluster frequency, calculated from the first two clusters evoked by a 4s-depolarizing current pulse (white bars) increased with depolarization of the membrane potential (correlation coefficient: R^2= 0.993), and that the frequency of subthreshold oscillations (black bars) similarly increased with depolarization of the membrane potential (correlation coefficient R^2= 0.991). D, Histogram showing that the voltage-dependence of the intercluster frequency, calculated from the first two to three clusters evoked by a 4s-depolarizing current pulse, increased slightly with membrane depolarization (correlation coefficient R^2= 0.911). The junction potential was corrected.

Figure 7. I_h current blockade by ZD7288 profoundly affects electrophysiological properties of fast-firing and burst-firing neurons but not slow-firing and cluster-firing neurons. In a fast-firing cell, ZD 7288 (100 μM) totally blocked I_h current as shown by the instantaneous (open symbols) and steady-state (closed symbols) I-V plots (A) derived from voltage-clamp recordings of the membrane currents evoked by hyperpolarizing voltage steps applied from a holding potential of –50 mV before (squares) and during (circles) bath application of ZD 7288

(100 μM) (not shown). In the same neuron, ZD 7288 totally abolished the depolarizing sag induced by a hyperpolarizing current pulse (B, left panel) and decreased the mean firing rate in response to a depolarizing current pulse applied from –80 mV (B, right panel). In a burst-firing cell, ZD 7288 (100 μM) also induced a complete blockade of I_h current as shown by the instantaneous (open symbols) and steady-state (closed symbols) I-V plots (C), as well as a complete blockade of the depolarizing sag (D, left panel). In addition, ZD 7288 induced an increase of the delay at which rebound firing occurred, as well as a decrease of the instantaneous frequency calculated from the time interval between the first two spikes occurring in rebound firing (D, left panel). ZD 7288 finally decreased the mean firing rate of this burst-firing neuron when depolarized from –80 mV (D, right panel). In contrast**,** ZD 7288 (100 μM) induced a small blockade of the small I_h current in slow-firing (E) and cluster-firing (G) neurons, as shown by the instantaneous (open symbols) and steady-state (closed symbols) I-V plots derived from voltage-clamp recordings of the membrane currents evoked by hyperpolarizing voltage steps applied from a holding potential of –50 mV before (squares) and during (circles) bath application of ZD 7288 (100 μM) (not shown). In slow-firing neurons, ZD 7288 did not affect the membrane response to injection of hyperpolarizing current pulses (F, left panel), or their mean firing rate when depolarized from –80 mV (F, right panel). In the same way, ZD 7288 did not affect the membrane response to injection of hyperpolarizing current pulses in cluster-firing neurons (H, left panel), and more importantly, did not affect clustering of action potentials (H, right panel). (Vertical bars: 20 mV; horizontal bars: 200 ms).

Figure 8. I_h significantly contributes to the mean firing rate, the delay of occurrence of rebound firing, and the instantaneous frequency of rebound firing in fast-firing and burst-

firing neurons. A, ZD 7288 (100 μM) significantly decreased the mean firing rate of fast-firing (*t*-test, *p<0.01*) and burst-firing (*t*-test, *p<0.05*) neurons, but not of slow-firing neurons. B, ZD 7288 increased the delay of occurrence of rebound firing in fast-firing and burst-firing neurons, but not in slow-firing neurons. In burst-firing neurons, this effect was significantly more profound than in both fast-firing ($p<0.05$) and slow-firing ($p<0.001$) neurons. In fast-firing neurons, this effect of ZD was significantly greater than in slow-firing neurons ($p<0.05$). C, ZD 7288 decreased the instantaneous frequency of rebound firing in fast-firing and burst-firing neurons, but not in slow-firing neurons. In both fast-firing and burst-firing neurons, the effects of ZD 7288 were significantly different from the effect in slow firing neurons ($p<0.001$).

D, I_h current amplitude, determined for a hyperpolarizing voltage step from -50 to –120 mV, was plotted as a function of the amplitude of the depolarizing sag (rectification), measured for a hyperpolarizing current pulse inducing an initial hyperpolarization of the membrane to –95 mV, for each neuronal population. This plot shows a perfect linear correlation between these two parameters for each neuronal population ($r^2=0.9726$). E, The mean firing rate, determined for a depolarizing current pulse applied from –60 mV, was plotted as a function of the amplitude of the depolarizing sag for each neuronal population, showing a perfect linear correlation ($r^2=0.9968$) between these two parameters. F, The mean firing rate, determined for a depolarizing current pulse applied from –60 mV, was plotted as a function of the amplitude of the I_h current for each neuronal population, showing again a perfect linear correlation ($r^2=0.9879$) between these two parameters. These analyses showed that burst-firing exhibited the largest I_h current and depolarizing sag, correlated to the fastest firing rate; slow-firing neurons displayed the smallest I_h current and depolarizing sag, associated to the slowest firing rate; fast-

firing neurons were intermediate between burst-firing and slow-firing neurons for all three parameters.

Table 1: Electrophysiological properties of chemically identified neuronal populations in the rat medial septum – diagonal band complex.

Chemical phenotype	**ChAT-positive cells (n=14)**	**GAD67-positive cells (n=24)**		**ChAT & GAD67-positive cells (n=19)**			**VGLUT-positive cells (n=21)**
Electrophysiological profile	Slow-firing (n=14)	Burst-firing (n=12)	Fast-firing (n=12)	Burst-firing (n=10)	Fast-firing (n=6)	Slow-firing (n=3)	Slow/Cluster-firing (n=21)
F_{MAX} (Hz)	16.3 ± 1.6 [a, c]	36.7 ± 5.5 [d, e, f, g]	23.9 ± 4.1	28.3 ± 1.9 [l]	23.6 ± 0.8	19.1 ± 5.9	18.6 ± 2.3
F_{STEADY} (Hz)	6.3 ± 0.6 [a, b, c]	16.3 ± 2.4 [e, f, g]	12.3 ± 1.6 [i]	13.3 ± 2.7 [j, k, l]	8.0 ± 1.2	5.5 ± 1.0	6.4 ± 0.7
Mean firing rate (Hz)	7.8 ± 0.6 [a, b, c]	20.5 ± 2.4 [d, e, f, g]	13.4 ± 1.9 [h, i]	17.5 ± 2.2 [j, k, l]	10.8 ± 0.8	7.5 ± 0.3	7.2 ± 0.7
AHP amplitude (mV)	7.4 ± 0.7 [c]	5.1 ± 0.7 [f, g]	6.6 ± 1.1 [i]	4.2 ± 0.6 [j, k, l]	6.99 ± 0.8	8.7 ± 1.2	7.7 ± 0.8
AHP duration (ms)	216.1 ± 15.3	169.0 ± 19.0 [f, g]	190.9 ± 20.4	171.7 ± 34.3 [k, l]	193.7 ± 17.9	250.0 ± 14.6	245.1 ± 29.7
Amplitude sag (mV)	3.0 ± 0.6 [a, b, c]	11.2 ± 1.2 [d, e, f, g]	6.6 ± 1.3 [h, i]	10.6 ± 1.5 [j, k, l]	6.11 ± 0.4	4.5 ± 1.8	2.76 ± 0.2
Amplitude Ih (pA)	29.4 ± 5.5 [a, c]	54.3 ± 8.6 [f, g]	42.6 ± 7.6	53.1 ± 10.9 [k, l]	46.7 ± 9.8 [m]	22.8 ± 7.8	28.0 ± 2.9
Ih activation (T1/2, ms)	431.1 ± 30.1 [a, b, c]	212.6 ± 45.3 [f, g]	326.0 ± 61.2 [i]	245.6 ± 31.6 [k, l]	243.5 ± 69.4 [m, n]	495.7 ± 110.2	459.9 ± 25.6

Significant differences (P<0.05) are indicated: [a] ChAT-positive slow-firing versus GAD-positive burst-firing cells; [b] ChAT-positive slow-firing versus GAD-positive fast-firing cells; [c] ChAT-positive slow-firing versus ChAT & GAD-positive burst firing cells; [d] GAD-positive burst firing versus GAD-positive fast-firing cells; [e] GAD-positive burst firing versus ChAT & GAD fast-firing cells; [f] GAD-positive burst-firing versus ChAT & GAD-positive slow-firing cells; [g] GAD-positive burst-firing versus VGLUT-positive slow/cluster-firing cells; [h] GAD-positive fast-firing versus ChAT & GAD-positive burst-firing cells; [i] GAD-positive fast-firing versus VGLUT-positive slow/cluster-firing cells; [j] ChAT & GAD-positive burst-firing versus ChAT & GAD-positive fast-firing cells; [k] ChAT & GAD-positive burst-firing versus ChAT & GAD-positive slow-firing cells; [l] ChAT & GAD-positive burst-firing versus VGLUT-positive slow/cluster-firing cells; [m] ChAT & GAD-positive fast-firing versus ChAT & GAD-positive slow-firing cells; [n] ChAT & GAD-positive fast-firing versus VGLUT-positive slow/cluster-firing cells.

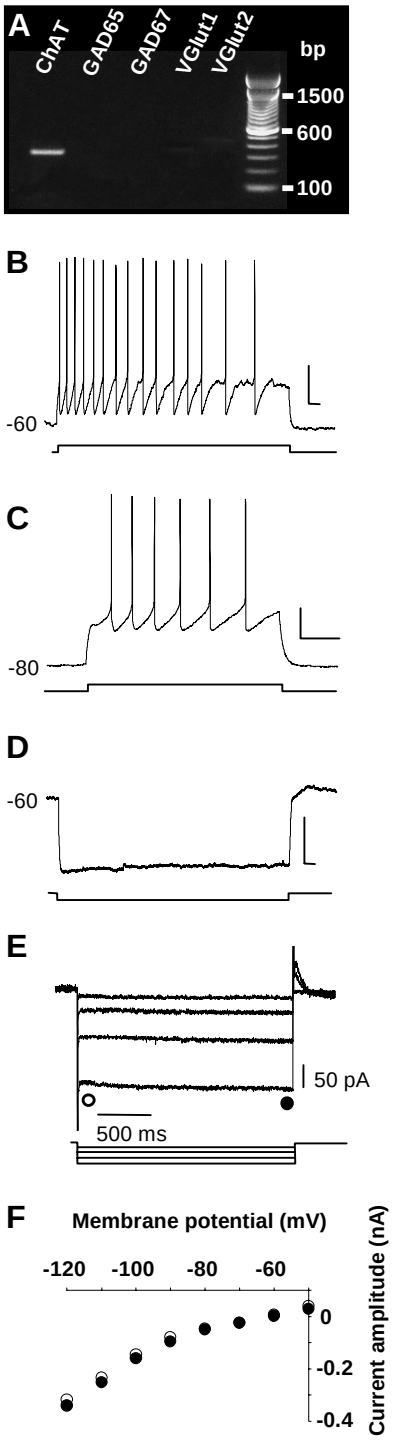
A
ChAT
GAD65
GAD67
VGlut1
VGlut2
bp
1500
600
100
B
-60
C
-80
D
-60
E
50 pA
500 ms
F
Membrane potential (mV)
-120
-100
-80
-60
0
-0.2
-0.4
Current amplitude (nA)

Figure 1

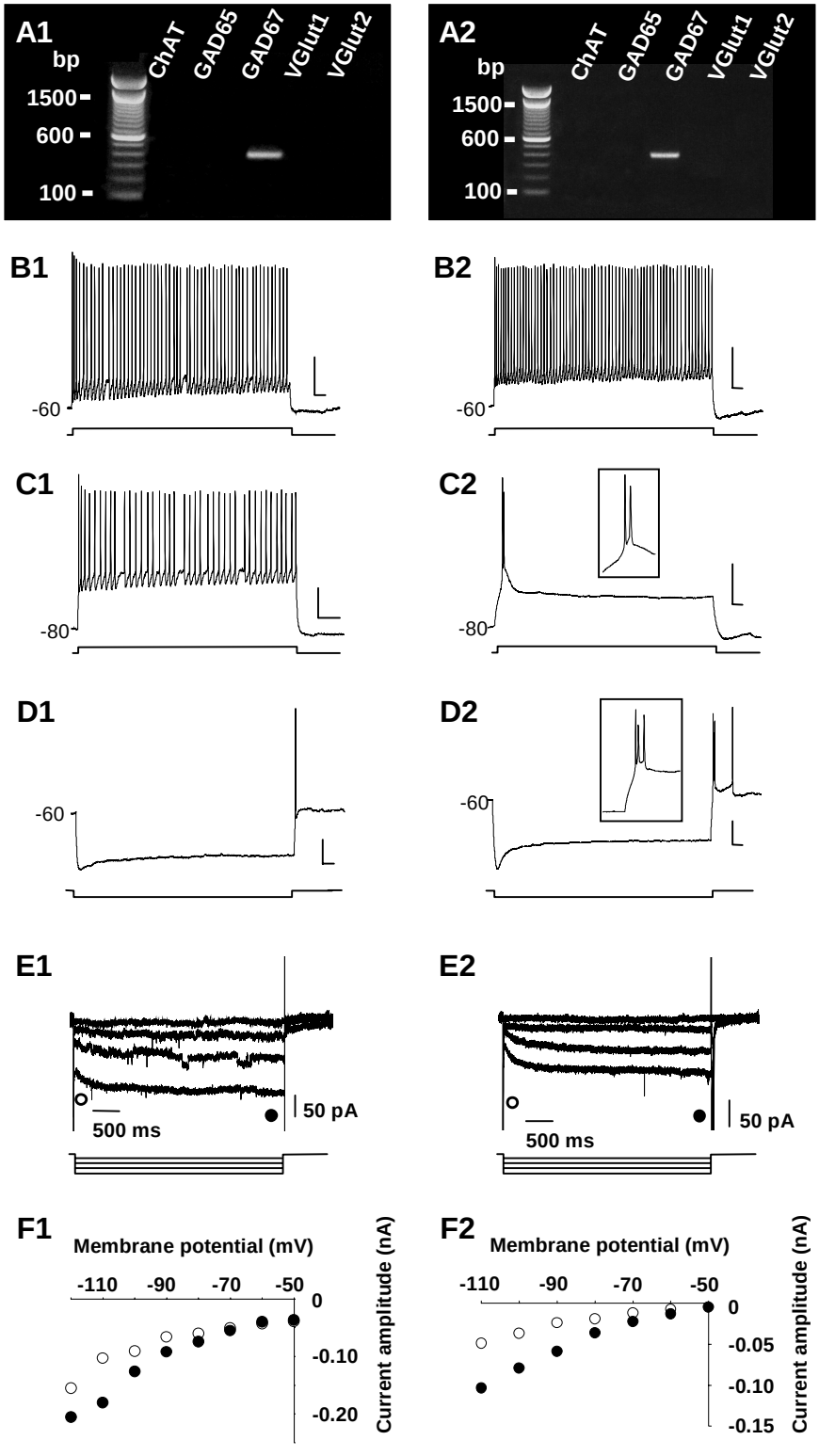
A1
bp
1500
600
100
ChAT
GAD65
GAD67
VGlut1
VGlut2
A2
bp
1500
600
100
ChAT
GAD65
GAD67
VGlut1
VGlut2
B1
-60
B2
-60
C1
-80
C2
-80
D1
-60
D2
-60
E1
50 pA
500 ms
E2
50 pA
500 ms
F1
Membrane potential (mV)
-110
-90
-70
-50
0
-0.10
-0.20
Current amplitude (nA)
F2
Membrane potential (mV)
-110
-90
-70
-50
0
-0.05
-0.10
-0.15
Current amplitude (nA)

Figure 2

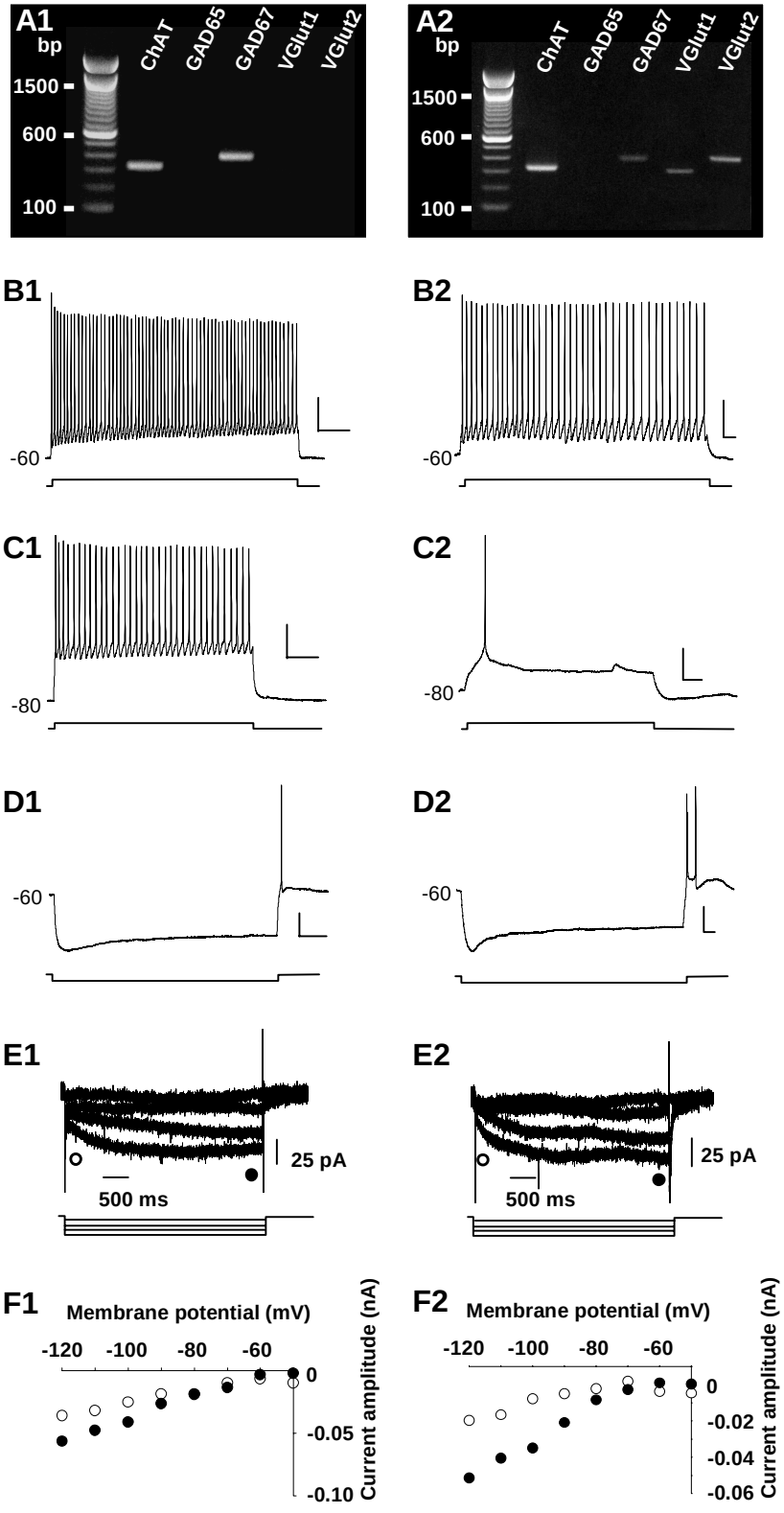
A1
bp
1500
600
100
ChAT
GAD65
GAD67
VGlut1
VGlut2
A2
bp
1500
600
100
ChAT
GAD65
GAD67
VGlut1
VGlut2
B1
-60
B2
-60
C1
-80
C2
-80
D1
-60
D2
-60
E1
25 pA
500 ms
E2
25 pA
500 ms
F1
Membrane potential (mV)
-120
-100
-80
-60
0
-0.05
-0.10
Current amplitude (nA)
F2
Membrane potential (mV)
-120
-100
-80
-60
0
-0.02
-0.04
-0.06
Current amplitude (nA)

Figure 3

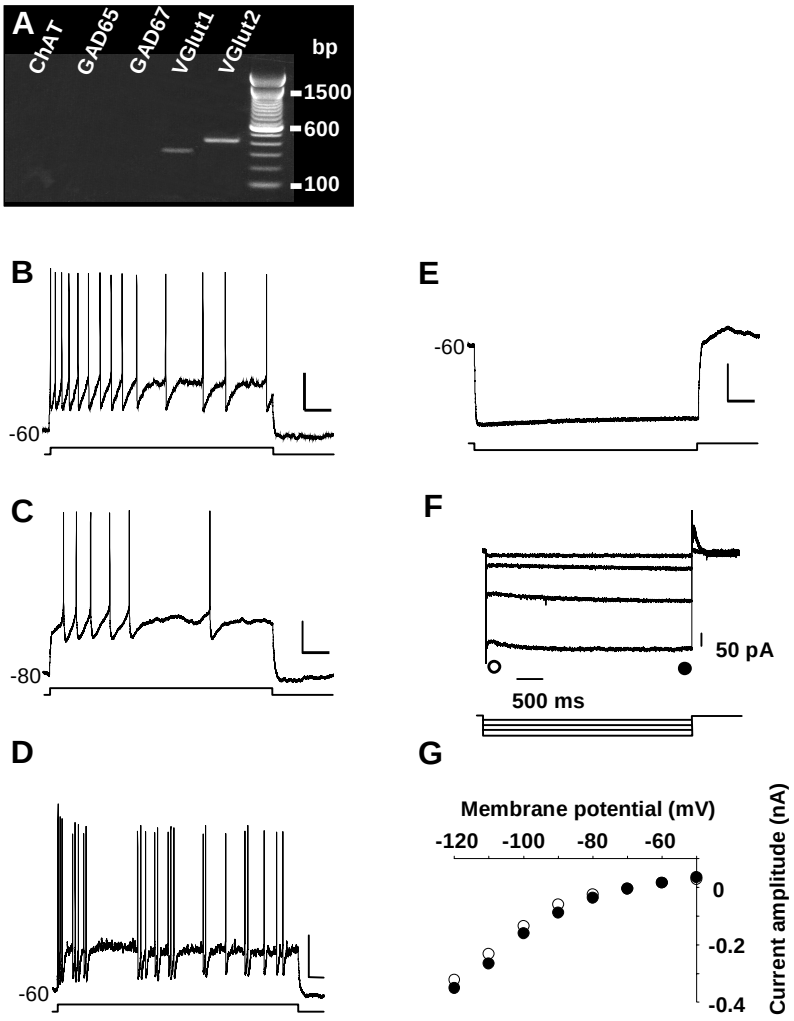
A
ChAT
GAD65
GAD67
VGlut1
VGlut2
bp
1500
600
100
B
-60
C
-80
D
-60
E
-60
F
50 pA
500 ms
G
Membrane potential (mV)
-120
-100
-80
-60
0
-0.2
-0.4
Current amplitude (nA)

Figure 4

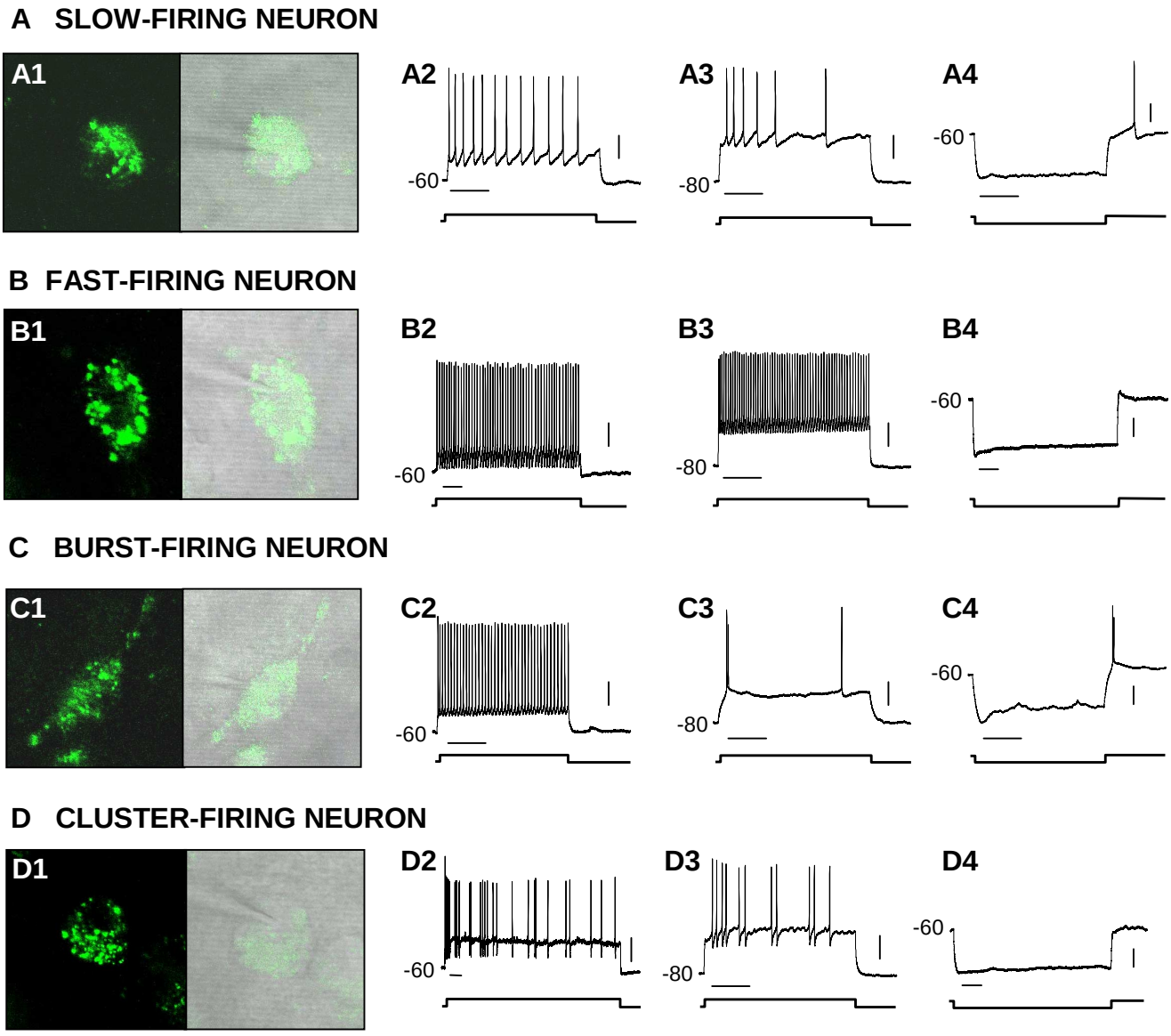
A SLOW-FIRING NEURON
A1
A2
A3
A4
-60
-80
-60
B FAST-FIRING NEURON
B1
B2
B3
B4
-60
-80
-60
C BURST-FIRING NEURON
C1
C2
C3
C4
-60
-80
-60
D CLUSTER-FIRING NEURON
D1
D2
D3
D4
-60
-80
-60

Figure 5

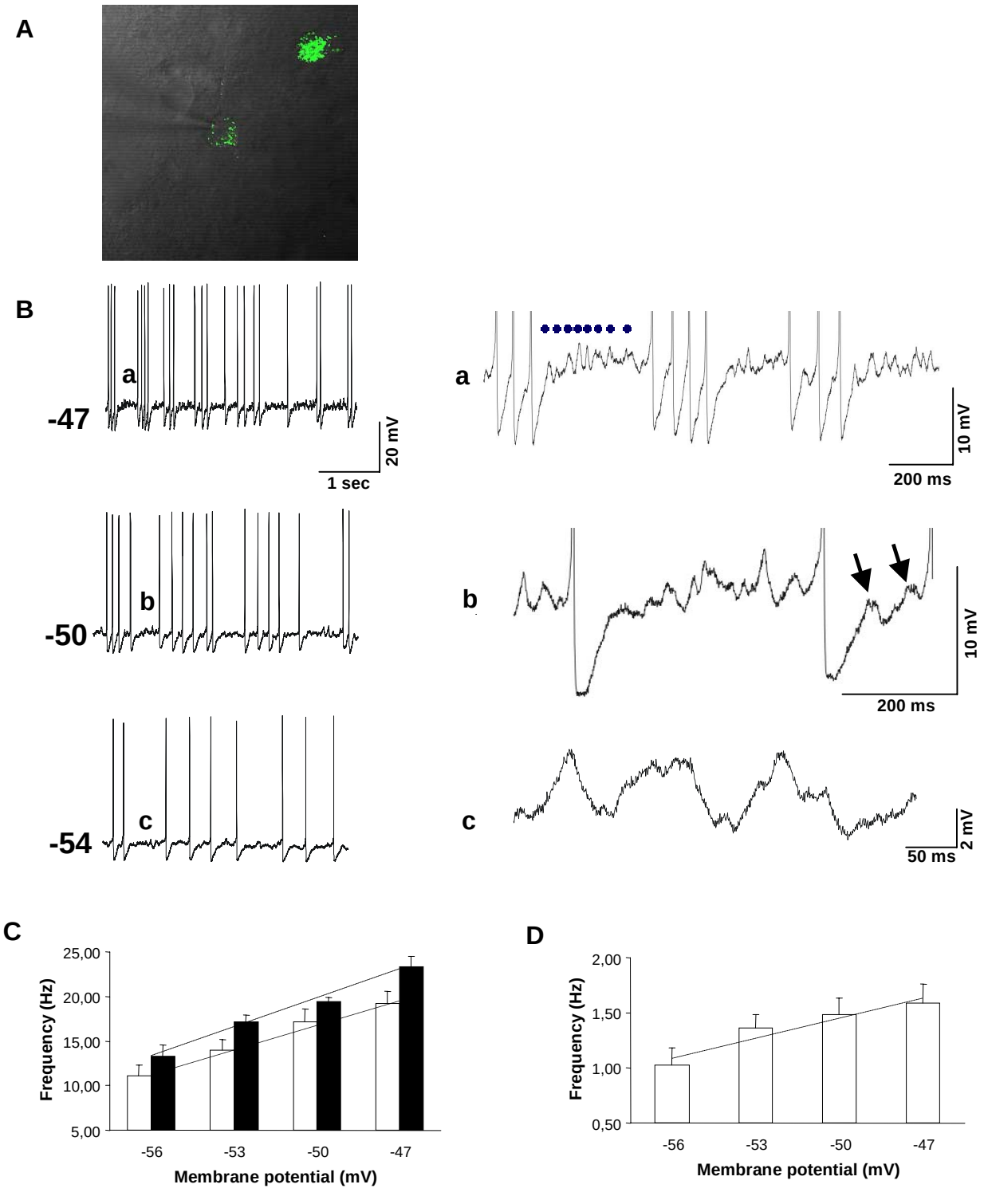
A
B
a
-47
20 mV
1 sec
b
-50
c
-54
a
10 mV
200 ms
b
10 mV
200 ms
c
2 mV
50 ms
C
Frequency (Hz)
25,00
20,00
15,00
10,00
5,00
-56
-53
-50
-47
Membrane potential (mV)
D
Frequency (Hz)
2,00
1,50
1,00
0,50
-56
-53
-50
-47
Membrane potential (mV)

Figure 6

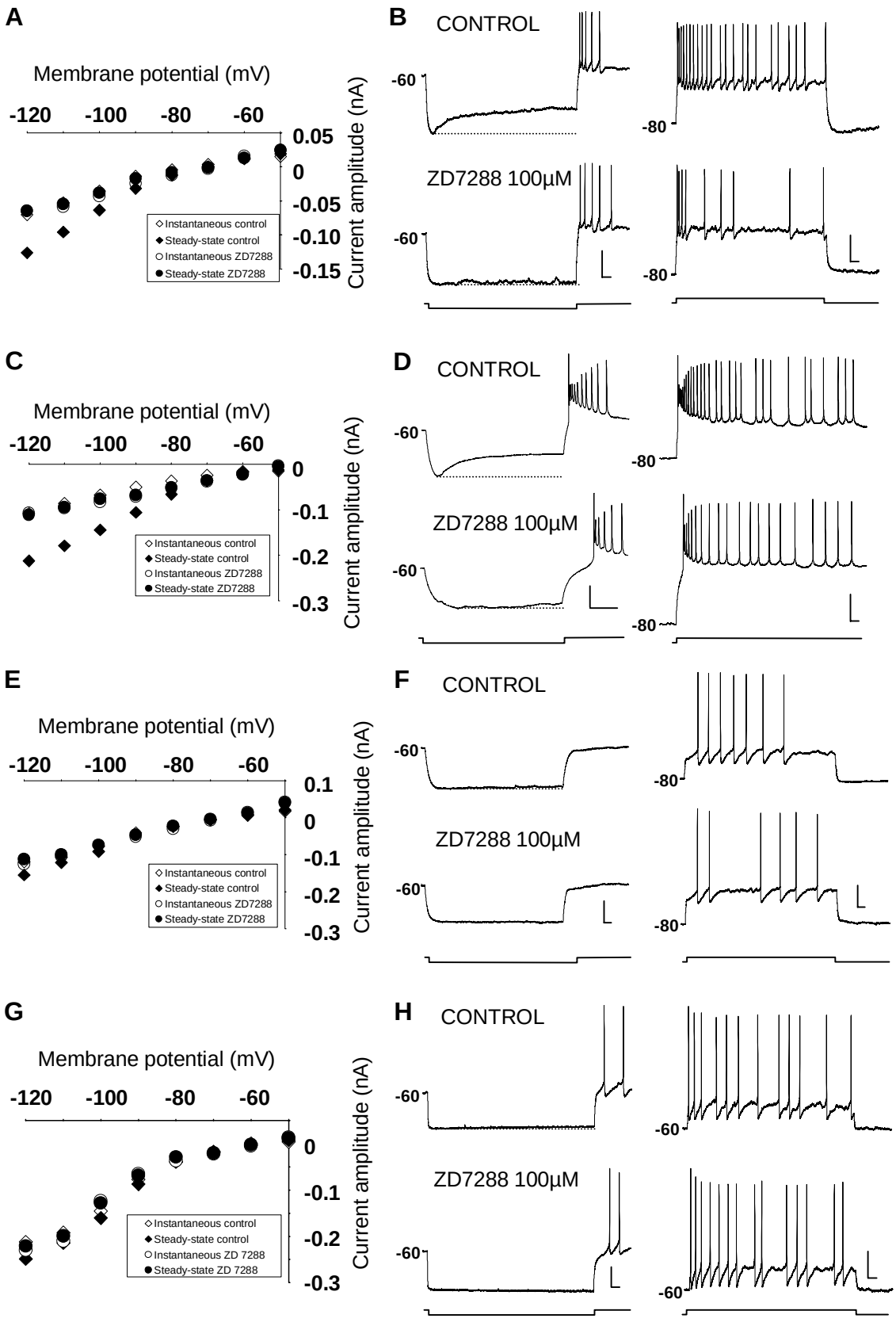
A
Membrane potential (mV)
-120
-100
-80
-60
0.05
0
-0.05
-0.10
-0.15
Current amplitude (nA)
Instantaneous control
Steady-state control
Instantaneous ZD7288
Steady-state ZD7288
B
CONTROL
ZD7288 100µM
-60
-80
C
Membrane potential (mV)
-120
-100
-80
-60
0
-0.1
-0.2
-0.3
Current amplitude (nA)
Instantaneous control
Steady-state control
Instantaneous ZD7288
Steady-state ZD7288
D
CONTROL
ZD7288 100µM
-60
-80
E
Membrane potential (mV)
-120
-100
-80
-60
0.1
0
-0.1
-0.2
-0.3
Current amplitude (nA)
Instantaneous control
Steady-state control
Instantaneous ZD7288
Steady-state ZD7288
F
CONTROL
ZD7288 100µM
-60
-80
G
Membrane potential (mV)
-120
-100
-80
-60
0
-0.1
-0.2
-0.3
Current amplitude (nA)
Instantaneous control
Steady-state control
Instantaneous ZD 7288
Steady-state ZD 7288
H
CONTROL
ZD7288 100µM
-60

Figure 7

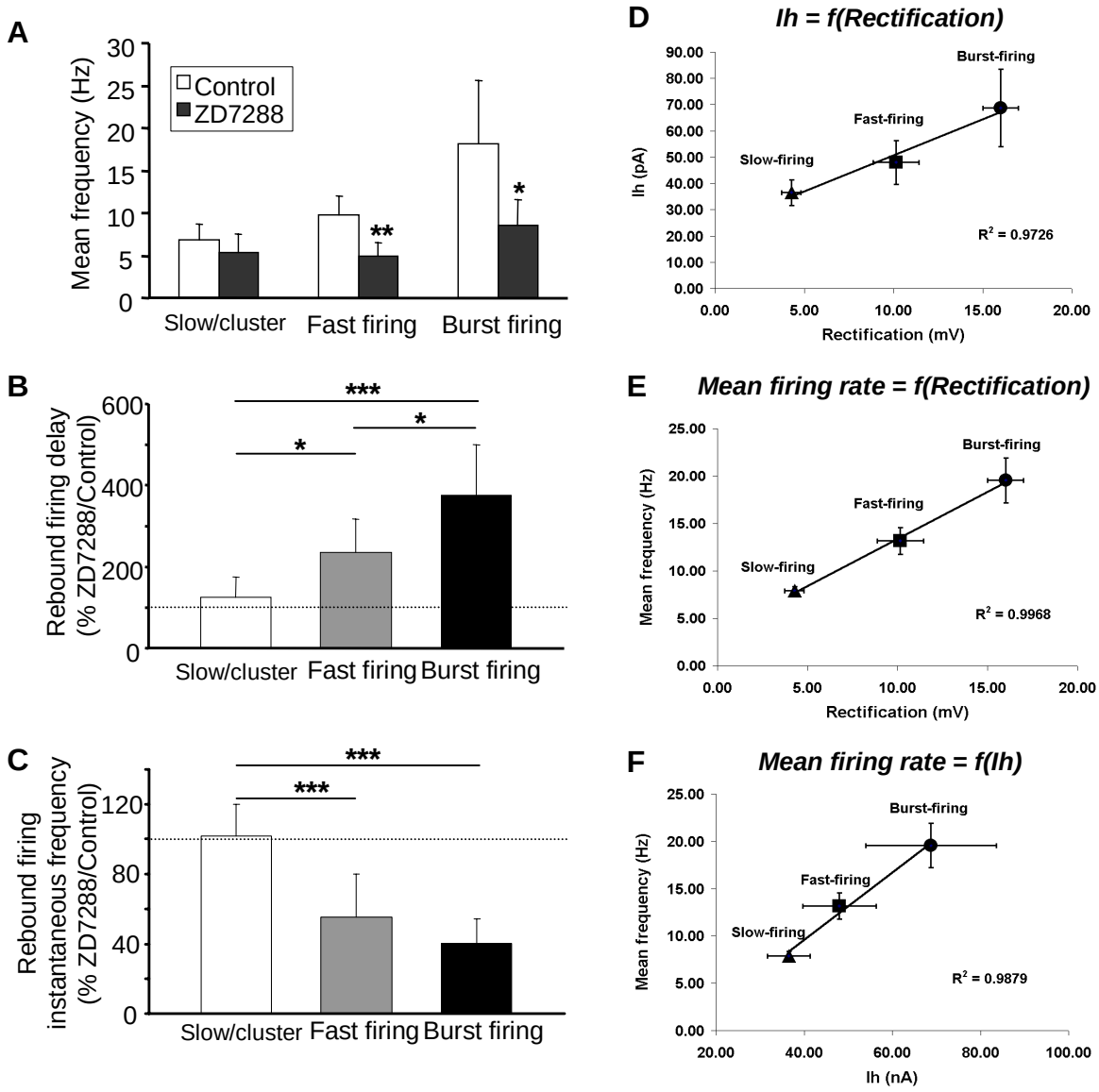
A
Mean frequency (Hz)
Control
ZD7288
Slow/cluster
Fast firing
Burst firing
B
Rebound firing delay (% ZD7288/Control)
C
Rebound firing instantaneous frequency (% ZD7288/Control)
D
Ih = f(Rectification)
Ih (pA)
Rectification (mV)
Slow-firing
Fast-firing
Burst-firing
R² = 0.9726
E
Mean firing rate = f(Rectification)
R² = 0.9968
F
Mean firing rate = f(Ih)
Ih (nA)
R² = 0.9879

Figure 8